Joint Centre for Mesoscale Meteorology, Reading, UK

Cold Frontal Structure derived from radar wind profilers

K. A. Browning
D. Jerrett
J. Nash
T. Oakley
N. M. Roberts

Internal Report No. 67

May 1997

Met Office Joint Centre for Mesoscale Meteorology Department of Meteorology
University of Reading PO Box 243 Reading RG6 6BB United Kingdom
Tel: +44 (0)118 931 8425 Fax: +44 (0)118 931 8791
www.metoffice.com

Designed and produced by the Met Office © Crown copyright 2001 01/0240 The Met Office logo is a registered trademark.

Revised May 1997

COLD FRONTAL STRUCTURE DERIVED FROM RADAR WIND PROFILERS

K. A. Browning[1], D. Jerrett[2], J. Nash[2], T. Oakley[2] and N. M. Roberts[1]

(1) Joint Centre for Mesoscale Meteorology, University of Reading, Reading, RG6 6BB, UK
(2) Meteorological Office, Bracknell, Berkshire, RG12 2SZ, UK

Colocated UHF and VHF wind profiler radars have been operated during the passage of a sharp cold front. The results demonstrate the utility of the profilers, in conjunction with a conceptual model, for identifying and quantifying many of the features commonly associated with such fronts: low-level and upper-level jets, rearward-sloping warm-conveyor-belt flow with underlying rear-inflow. The UHF radar detected much of the transverse circulation and also the vertical distribution of precipitation, including a possible region of evaporation associated with the dry rear-inflow jet. The VHF radar, in addition to extending the velocity measurements above the level of the precipitation, mapped the tropopause and, in particular, identified a tropopause fold the position of which corresponded to the origin of the rear-inflow jet detected by both profilers.

1. Introduction

A 2-month trial of a 915 MHz (UHF) radar wind profiler, a RADIAN LAP - 3000, was undertaken in early 1995. This was carried out alongside a 46.5 MHz (VHF) radar wind profiler, also refered to as an MST (Mesosphere Stratosphere Troposphere) radar, at Aberystwyth on the west coast of Wales. The normal use for a 915 MHz system in meteorology is as a clear-air boundary-layer wind profiler. However, such a system can also detect precipitation thereby enabling it to obtain wind profiles throughout much of the troposphere in the presence of precipitation. Gage et al (1994) have already demonstrated the utility of 915 MHz radar for observing deep convective systems in the tropics. Kotroni et al (1995) have shown its utility for observing mid-latitude frontal systems. The present article extends this demonstration by showing how the use of a conceptual model enables a forcaster to interpret the profiler data almost at a glance.

During the period of the trial, on 22 February 1995, a sharp ana-cold front was observed which produced heavy rain, severe wind gusts and lightning. The standard output of the 915 MHz radar wind profiler depicted in Figure 1 shows the temporal veer and decrease in low-level winds that accompanied the passage of the sharp surface cold front at 1345 UTC. (This main cold front is labelled 1 along the time axis of Figure 1; a much weaker secondary cold front, labelled 2, is discussed later). The frontal system was associated with an upper-level jet at 6 to 7 km. Figure 1 shows that the winds increased from 37.5 to 50 m s^{-1} above a sloping interfacial zone that separated these strong winds from the weaker veered flow below.

We shall show, by means of various standard forms of radar output, how useful a 915 MHz profiler can be in diagnosing various aspects of the frontal structure typical of this kind of cold front. Information about frontal

structure at heights above 2.5 km was also provided by the larger 46.5 MHz radar, as previously demonstrated for a rather similar radar by Larsen and Röttger (1982); however, many inferences can be made solely on the basis of the smaller 915 MHz system, especially regarding the tropospheric flow in the region of precipitation. Henceforth, for simplicity we shall refer to the two systems as the UHF and VHF radars, respectively.

2. The UHF and VHF wind profiling radars used in this study

The VHF wind profiler radar at Aberystwyth, as described by Slater et al (1991), is an MST facility owned and operated by the Natural Environment Research Council in conjunction with the Rutherford Appleton Laboratory and the University of Wales Aberystwyth. The antenna is a 20x20 Yagi phased array, operating at 46.5 MHz with a half-beam-width of 3.3 degrees. The radar is capable of producing up to 15 oblique beams plus a vertical beam. However, processing was performed on only three beams for this study: one vertical beam and two oblique beams. The oblique beams were at an angle of 6 degrees from vertical, in the directions northeast and southeast. During the period from February to April 1995 the radar was operated continuously, producing a wind profile every twelve minutes with a vertical resolution of 150 m in the height range 2-20 km.

The UHF radar is a RADIAN LAP-3000. This is a 4-panel antenna, 915 MHz radar operating in three-beam mode: vertical, north and east at 23.5 degrees from zenith, with a 10 degree half-beam-width. The height range sampled in dry conditions was 120 m to 3 km, increasing to 7 km in precipitation, with a vertical resolution of 100 m. The LAP-3000 radar was also operated continuously for the two months. For the event reported in this paper data processing was configured to produce wind profiles every 15 minutes. If was found that in rapidly changing situations a 15 minute averaging period was best able to follow the meteorological changes that were occurring without too much compromise on quality caused by the smallness of the number of wind measurements required for consensus. The

minimum number of measurements required for consensus was 3, with 5 being typical.

3. The synoptic context

Figure 2 shows the synoptic situation at 1500 UTC on 22 February 1995, 1½ hours after the primary surface cold front (SCF) passed over the wind profilers at Aberystwyth. Figure 2(a) shows a combined display of weather radar network data and Meteosat infrared (IR) and water vapour (WV) imagery superimposed on the subjectively analysed msl pressure pattern. Figure 2(b) shows the corresponding analysis of features of the flow referred to later, with the location of Aberystwyth shown by the letter A. Data from the Aberystwyth profilers for the corresponding period, 1100 to 2200 UTC, are presented in Section 4.

The thin band of dark blue radar echo in Figure 2(a) stretching from the tip of southwest England to northeast England corresponds to a rather 2-dimensional narrow cold-frontal rainband (NCFR) symptomatic of line convection along the SCF of the main cold front, referred to as CF 1. Line convection is an indicator of a sharp SCF and this was supported by detailed analysis on this occasion (not shown). The NCFR is embedded within a wide cold-frontal rainband (WCFR) associated with a belt of lighter rain (pale blue) over a width of about 100km. Some 100km behind this is another ragged band of shower echoes associated with a second (minor) cold front (CF 2). Both cold fronts are situated beneath what Weldon (1979) calls a baroclinic leaf cloud stretching from just west of southwest England to Scotland. This is distinct from another, almost precipitation-free, leaf cloud over central England and the North Sea, the rear edge of which is just ahead of the SCF associated with CF 1.

The frontal structure seen in Figure 2(a) had sharpened significantly during the 1¼ hours following the passage of CF 1 over Aberystwyth at 1345 UTC : before that there had been little sign of line convection. Numerical

model products (not shown) indicate that the sharpening of the front was accompanied by the approach of an intrusion of dry air of low wet-bulb potential temperature (θ_w) from the rear - the so-called dry intrusion (Browning 1996). This was associated with a dry zone in the WV imagery (green area in Figure 2(a)) which had been encroaching upon the tail of the leaf cloud.

Evidence from the wind profiling radars (shown later) indicates that the dry intrusion undercut the leaf cloud to give what is often referred to as a rear-inflow jet (Smull and Houze 1987). This is believed to have played a major role in the development of the overall frontal circulation. Figure 2(b) shows a schematic interpretation of the low-θ_w dry-intrusion flow (green arrow) beneath the high-θ_w, warm-conveyor-belt (WCB) flow (red arrow) responsible for the generation of the leaf cloud. The main point about Figure 2(b), is that it implies a transverse-front circulation (dry-intrusion flow down and to the east : WCB flow upwards and to the west relative to the frontal system) superimposed on an overall component of flow parallel to the cold-frontal zone.

4. The frontal structure as revealed by the wind profiling radars

We now present a set of radar-profiler time-height diagrams (Figures 3-6) for the period 1100 to 2200 UTC during the west-east passage of the cold-frontal system over Aberystwyth and we interpret them in terms of the conceptual model of an ana-cold front (Browning 1990). The front-normal component of the frontal propagation velocity was 15 m s^{-1} (54 km h^{-1}) from 302 deg, so that the 11-hour records plotted in Figures 3-6 correspond to a distance of about 600 km resolved perpendicular to the front (ie the ratio of the vertical to horizontal scale is about 1 to 30). We shall relate the radar-derived frontal structure to the patterns of cloud and rain shown in Figure 2(a) and to the airflow pattern sketched in Figure 2(b). We shall schematically identify key features in each of the cross-sections and then assemble them together in Figure 7.

Figures 3 (a and b) show wind-component information combined from both the UHF and VHF profilers. The information below the dotted line is from the UHF system and that above the line is from the VHF system. As is clear from the later Figure 5, the VHF system does not provide information below 2.5 km agl, although it provides abundent information at high levels, including levels far above those relevant to the present study. On the other hand the UHF system, whilst failing to observe the upper levels, can provide information down as low as 120 m agl. Comparisons (not shown) indicate good agreement between the two systems at levels where they both provide measurements. More generally, comparison of the wind speed measurements by the UHF system with measurements from over one hundred radiosondes launched throughout the trial period show near zero bias. Over the same period the wind speed measurements by the VHF system had a bias of about -1 m s^{-1}. Random errors in wind measurements are estimated to be less than 1 m s^{-1} for orthogonal wind components for the UHF measurements, and between 1.5 and 2 m s^{-1} for the present mode of VHF operation (Jerrett 1996). Similar accuracies have been reported by Martner et al (1993).

The along-front and across-front wind components shown in Figures 3(a) and (b), respectively, are resolved with respect to a frontal orientation of 212-032 deg. Figure 3(a) shows the strong parallel-front flow (green) associated with the warm parts of the frontal system, separated from weaker flow beneath and to the west by a shear zone sloping at about 1 in 40 (the slope is inferred from the time record assuming the front retained a constant shape as it travelled overhead). Parts of the strong flow specifically associated with the cross-frontal circulation described shortly, notably the upper-level jet maximum (J) and an ill-defined low-level jet (LLJ), are labelled in Figure 3(a) and in the composite diagram shown later in Figure 7.

Figure 3(b) shows the transverse circulation associated with CF 1. We have highlighted it here (and in Figure 7) by a pair of arrows, one drawn with continuous thick lines and the other with thin. The former corresponds to the WCB air, originating mainly from the boundary layer ahead of the SCF, which rises in the line convection at 1345 UTC and then ascends slantwise towards J. This arrow represents just the ascending portion of the rearward flow and is terminated near J, at a location that corresponds to the western boundary of the leaf cloud as seen in the satellite imagery (refer ahead to Figure 7). The passage of the line convection was accompanied by low-level cyclonic shear and convergence which show up in Figures 3(a) and 3(b) respectively, as green-blue and orange-blue time transitions. The other limb of the transverse circulation, denoted by the continuous thin-lined arrow in Figure 3(b), is the rear-to-front relative flow, or rear-inflow jet. Such a flow was a feature of the early Doppler radar results of Browning and Harrold (1970) and has since been shown to be a common and dynamically important feature by Smull and Houze (1987). This rear-inflow jet corresponds to part of the dry-intrusion flow shown in Figure 2(c).

Beneath the main rear-inflow jet there is some evidence of a smaller transverse circulation associated with CF 2. This is represented tentatively in Figure 3(b) (and in Figure 7) by dashed arrows. The white areas in Figure 3 are regions where the UHF profiler has failed to find consensus and has not calculated a wind. This failure is due to rapid changes in wind velocity between observations in one beam direction and another and are coincident with times of precipitation at the surface measured by rainguage. The regions at 1345 and 1600 UTC correspond to the convective precipitation occurring at the surface positions of CF 1 and CF 2, respectively (see Figure 2(a)). The convection at the first of these lines (1345 UTC) is an integral part of the transverse circulation represented by the solid-line arrows. The convection associated with CF 2 appears to have a rather similar relationship to the transverse circulation represented by the dashed arrows.

Figure 4 depicts the distribution of reflectivity for the UHF profiler. At low levels some of the echo is from the clear air, but during the passage of the cold front it is mainly the effect of precipitation particles in increasing the signal-to-noise ratio that accounts for the detection of echoes significantly above 6km. A particularly significant feature, is the layer of minimum reflectivity emphasized by the slanting dashed line in Figure 4. This is thought to be due to evaporation of ice particles in descending through a 1-km layer while falling from the rearward-ascending WCB associated with CF 1 into the rear-inflow jet.

Where the cold air of the rear-inflow jet associated with the dry intrusion penetrates to the ground, other studies have shown that it behaves rather like a density current (eg Carbone 1982). Part of such a density current close to the ground returns rearwards as an undercurrent but most of it, as it nears the SCF, ascends within the density-current head and then rises along with the WCB air in the region of rearward-sloping ascent. The along-front wind component of the air in the rear-inflow jet decreases as it approaches the ground and the smallness of this component is preserved for a while as this flow mingles with the region of rearward-sloping WCB air. This is evident as the blue finger highlighted by a small arrow in Figure 3(a). A similar behaviour was noted by Browning and Harrold (1970).

Figure 5, depicting reflectivity from the VHF system provides two main kinds of information : weak echo layers above 6 km and multiple relatively strong echoes below 5 km. The weak layers of maximum reflectivity located above 6 km are due to Bragg scattering from refractive index inhomogeneities caused by small-scale temperature fluctuations at the tropopause. As shown by Vaughan et al (1995) these layers are a useful indication of tropopause height. Before 1500 UTC the tropopause is a two-layered feature. Between 1500 and 1800 UTC, Figure 5 shows the tropopause as a simple entity which, as shown later in Figure 7, bounds the upper-level jet and marks the upper limit of the cloud leaf associated with the ascent of WCB air at CF 1. (A

possible alternative interpretation is that the tropopause remains just below 9 km from 16 UTC until 19 UTC) Between 1800 and 1900 UTC, however, the tropopause folds strongly downwards. When the tropopause is plotted together with the rear inflow jet (as in Figure 7), it suggests a connection between these two features. As noted in many other studies, extruded stratospheric air probably accounts for some of the dry-intrusion air that descends in the rear-inflow jet.

The relatively intense echo layers below 5 km in Figure 5 are due to refractive index inhomogeneities caused mainly by humidity gradients. Early and late in the time-section these are irregularly disposed and are likely to be due to disorganized convection. During the passage of the frontal system from 1400 to 1800 UTC, however, these echoes tend to become organized as inclined layers with slopes of about 1 in 40. They probably represent the sheared boundaries between opposing moist and dry laminae. The best-defined echo layer (drawn dashed in Figure 5) corresponds to the base of the dry rear-inflow jet associated with CF 1 (see continuous thin-lined arrow in Figure 3(b)).

The wind-profiler cross-section in Figure 6 shows airflow vectors derived by combining the front-relative transverse-wind components from Figure 3(b) with the vertical air velocities observed directly from the vertical scans with the VHF profiler (not shown). Vertical air velocities derived from a VHF profiler can be contaminated by the terminal fallspeed of precipitation, eg. double peaks in spectrum (Yoe and Larsen 1992), but the precipitation intensity in the present case was usually too small for this to be a major problem. The profiler is sited in a hilly region on the west coast of Wales and so it is necessary to interpret the vertical air motion with great caution. Local topographically-induced effects are liable to produce vertical motions unrepresentative of (and sometimes larger than) those associated with the frontal circulation. Nevertheless, some features of the larger-scale-flow, notably the rearward-slanting ascent associated with CF 1 and the underlying

descent associated with its rear-inflow jet, do appear to be represented. The former shows a consistent area of ascent of up to about 50 cm s^{-1}. The latter shows a region of more variable descent of up to 50 cm s^{-1}. A few more extreme values occur but may be spurious. Elsewhere, in the warm air ahead of CF 1 and in the cold air behind CF 2, there is a predominance of tropospheric ascent. General ascent in the cold air is not to be expected; however, the cold air was convectively unstable and so the observed ascent may indicate the profiler site as a preferred region for triggering convection as the westerly flow comes inland.

5. Synthesis and concluding remarks

Figure 7 is a schematic diagram representing the structure of the vigorous cold frontal system that crossed Wales on 22 February 1995. It has been derived using data from colocated UHF and VHF radar wind profilers, interpreted in the context of satellite imagery and weather radar data. The figure brings together various features that are highlighted individually in the set of cross-sections in Figures 3 to 6. The principal feature, which can be confidently inferred from either profiler alone, is the transverse circulation associated with the primary cold front, CF 1. The existence of a weaker circulation associated with a secondary cold front, CF 2, is suggested but is less certain.

The CF 1 circulation depicted in Figure 7 is similar to that shown in the early Doppler radar studies of Browning and Harrold (1970). As summarized in the conceptual model shown in Figure 8.27(b) of Browning (1990), the main circulation consists of an extrusion of boundary-layer air via line convection followed by its rearward-sloping ascent (red arrow in Figure 2(b)). Beneath the latter there is a stratospheric extrusion associated with a rear-inflow jet. The rear-inflow jet corresponds to a dry intrusion (green arrow in Figure 2(b)) that originates at the tropopause fold in a region detectable as a dry zone in Meteosat water vapour imagery (green area in Figure 2(a)). Profiler observations show that rear-inflow jets occur in association with

mesoscale convection systems as well as with cold fronts (Ralph et al 1995). Rear-inflow jets have been studied extensively by Smull and Houze (1987) and Yang and Houze (1995). When, as in the present case, the maximum rear-to-front velocity is embedded deep within the precipitation region, they suggest that this maximum is attributable in large part to the cooling effect of evaporating ice particles (Clough and Franks 1991). In the present study we believe the evaporative cooling was enhancing the pre-existing synoptic-scale rear-to-front flow associated with the dry intrusion.

Acknowledgement

The Joint Centre for Mesoscale Meteorology is supported by the Meteorological Office and the Department of Meteorology, University of Reading

References

Browning, K. A. (1990). Organization of clouds and precipitation in extratropical cyclones. In *Extratropical cyclones : the Erik Palmén Memorial Volume,* (Newton C W and Holopainen E. O., eds), 129-153, Am. Meteorol. Soc., Boston, MA.

Browning, K. A. (1996). Some questions regarding the dry intrusions associated with extratropical cyclones. In *Proc. 7th Conf. On Mesoscale Processes, 9-13 Sept, Reading, UK,* Am. Meteorol. Soc, Boston, MA.

Browning, K. A. & Harrold, T. W. (1970). Air motion and precipitation growth at a cold front, *Q. J. R. Meteorol Soc.,* **96**, 369-389.

Carbone, R. E. (1982). A severe frontal rainband. Part I: Stormwide hydrodynamic structure. *J. Atmos. Sci.,* **39,** 258-279.

Clough, S.A. & Franks, R.A.A. (1991). The evaporation of frontal and other stratiform precipitation. *Q.J.R.Meteorol Soc.,* **117**, 1057 - 1080.

Gage, K. S., Williams, C. R. & Ecklund, W. L. (1994). UHF wind profilers : a new tool for diagnosing tropical convective cloud systems. *Bull. Am. Meteorol. Soc.,* **75,** 2289- 2294.

Jerrett, D. (1996). Results from a three month radio-sonde, MST radar and LAP-3000 intercomparison trial at Aberystwyth, Wales. Proceedings of the seventh workshop on technical and scientific aspects of MST radar, Hilton Head Island, South Carolina, USA, 7-11 Nov. 95, pp 170-173.

Kotroni, V., Lagouvardos, K. & Petitdidier, M. (1995). A comparison of wind profiler and sounding observations during a frontal event *Int. J. of Remote Sensing,* **16,** 1685-1695.

Larsen, M. F. & Röttger, J. (1982). VHF and UHF Doppler radars as tools for synoptic research. *Bull. Am. Meteorol. Soc.,* **63,** 996-1008.

Martner, B.E., Wuertz, D.B., Stankov, B.B., Strauch, R.G., Westwater, E.R., Gage, K.S., Ecklund, W.L., Martin, C.L. and Dabberdt, W.F. (1993). An evaluation of wind profiler, RASS, and Microwave radiometer performance. *Bull. Am. Met. Soc.*, **74**, 599-613.

Ralph, F.M., Neiman, P.J., van de Kamp, D.W. & Law,D.C.,(1995).Using spectral moment data from NOAA's 404 - MHz radar wind profilers to observe pricipitation. *Bull. Am. Meteorol. Soc.*, **76**, 1717-1739.

Smull, B. F. & Houze, R. A., Jr. (1987). Rear inflow in squall lines with trailing stratiform precipitation. *Mon. Wea. Rev.,* **115,** 2869-2889.

Slater, K (1991). Overview of the MST radar at Aberystwyth. Proc. Of Fifth Workshop on Technical Aspects of MST Radar, pp479-482.

Vaughan, G., Howells, A. & Price, J. D. (1995). Use of MST radars to probe the mesoscale structure of the tropopause. *Tellus,* **47A,** 759-765.

Weldon, R. B. (1979). Satellite training course notes. Part IV. Cloud patterns and upper air wind field. United States Air Force, AWS/TR - 79/DO3.

Yang, M-J. & Houze, R. A., Jr. (1995). Sensitivity of squall-line rear inflow to ice microphysics and environmental humidity. *Mon. Wea. Rev.,* **123,** 3175-3193.

Yoe, J.G. & Larsen, M.F. (1992). VHF wind- profiler data quality and comparison of methods for deducing horizontal and vertical air motions in a mesoscale convective storm. *J. Atmos. Oceanic Technol.* **9**, 713-727.

Figure captions.

Figure 1. Observed winds produced by the LAP-3000 UHF wind profiler radar located at Aberystwyth (see "A" in Figure 2) during the period 11-22 UTC on 22 February 1995. Each full wind barb denotes a speed of 10 m s^{-1} ; a solid flag denotes 25 m s^{-1}. The times of surface cold fronts (SCF) 1 and 2 are indicated as '1' and '2'.

Figure 2. Synoptic context showing cold-frontal system over British Isles at 1500 UTC, 22 February 1995. "A" marks the location of Aberystwyth.

(a) Meteosat imagery (infrared: cold cloud tops, white; warm cloud tops, dark grey. Water vapour dry zone, green). Radar-derived precipitation intensity (Heavy rain (≥4mm h^{-1}) , dark blue; light rain, pale blue). Isopleths represent msl pressure at 4-mb intervals.

(b) Schematic system-relative flow analysis and surface frontal analysis (omitting cold front 2 for simplicity) superimposed on infrared imagery (warm cloud deleted to de-emphasize the non-precipitating cloud area to the east of the main cold front, CFl).

Figure 3(a). Composite plot from UHF and VHF profilers of the along-front (212-032 deg) wind component showing the upper-level jet (J) at 6½ km at 1730 UTC and a low-level jet (LLJ) at 2 km at 1300 UTC. Above the dotted line the winds were obtained from the VHF profiler; below the line the values shown were obtained mainly from the UHF profiler. The small arrow is referred to in the text.

Figure 3(b). Same as Fig. 3(a) but showing the cross-frontal component (resolved along 302-122 deg) of the flow relative to the front. The area coloured red which is highlighted by a bold arrow shows the warm-conveyer-belt air flowing rearwards (and up) the frontal surface associated with cold front 1, with the dry descending air behind (blue

area highlighted by the thinner arrow). The dashed arrows represent flows probably associated with the minor cold front, CF2.

Figure 4. Signal-to-Noise Ratio from the LAP-3000 UHF profiler. SNR is a measure of reflectivity. High SNR's can be seen extending above 5 km in the main precipitation area from about 13 to 17 UTC. The area of low SNR highlighted by the dashed line is indicative of evaporation in the 1-km layer above it due to dry descending air in the rear-inflow jet.

Figure 5. Signal Power from the MST VHF profiler. Signal power is proportional to reflectivity. The slope of the main frontal surface is indicated by the inclined regions of high signal between 14 and 18 UTC, caused mainly by vertical humidity gradients in the lower troposphere. In the upper troposphere vertical temperature gradients are the dominant scattering mechanism showing, for example, a well defined tropopause (thin line) descending from 8.5 km at 15 UTC to around 8 km at 17 UTC. System performance falls off below about 2.5 km.

Figure 6. Front-relative velocity cross-section (resolved along 302-122 deg) through the front derived from the MST VHF system. The vector arrows have been scaled to show the vertical angle of the air motion relative to the frontal surface and hence the vertical velocity scale is different from the horizontal scale. The situation is complex but the rearward flow of warm-conveyor-belt air up the frontal surface and the descent associated with the rear-inflow jet are apparent.

Figure 7. Synthesis of features identified in all previous figures. CF = cold front, WCB = warm conveyor belt, LLJ = low-level jet, WV = satellite water vapour channel, and Trop = tropopause.

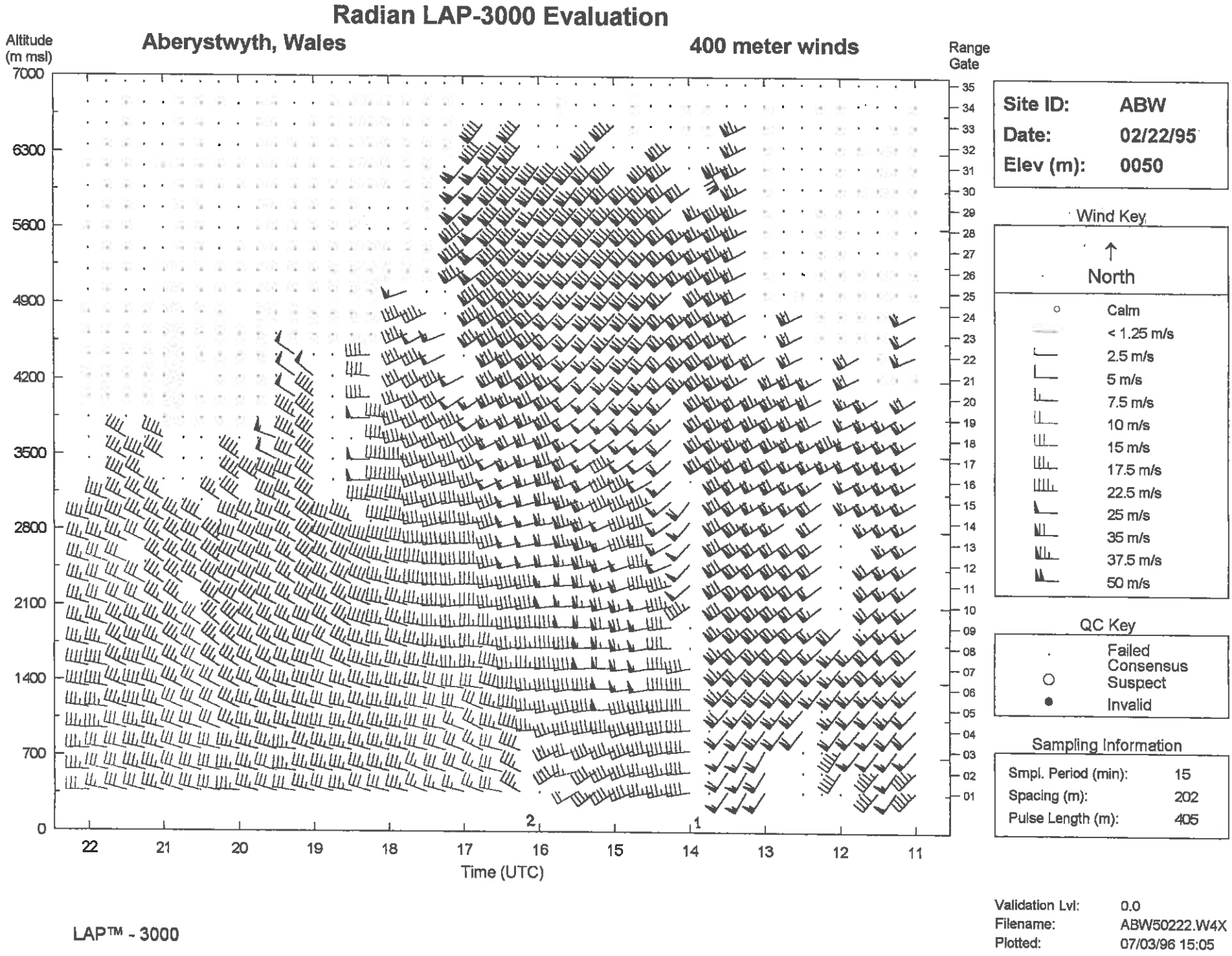
Radian LAP-3000 Evaluation
Aberystwyth, Wales
400 meter winds
Altitude (m msl)
7000
6300
5600
4900
4200
3500
2800
2100
1400
700
0
Range Gate
35
34
33
32
31
30
29
28
27
26
25
24
23
22
21
20
19
18
17
16
15
14
13
12
11
10
09
08
07
06
05
04
03
02
01
22
21
20
19
18
17
16
15
14
13
12
11
Time (UTC)
2
1
Site ID: ABW
Date: 02/22/95
Elev (m): 0050
Wind Key
North
Calm
< 1.25 m/s
2.5 m/s
5 m/s
7.5 m/s
10 m/s
15 m/s
17.5 m/s
22.5 m/s
25 m/s
35 m/s
37.5 m/s
50 m/s
QC Key
Failed Consensus
Suspect
Invalid
Sampling Information
Smpl. Period (min): 15
Spacing (m): 202
Pulse Length (m): 405
Validation Lvl: 0.0
Filename: ABW50222.W4X
Plotted: 07/03/96 15:05
LAP™ - 3000

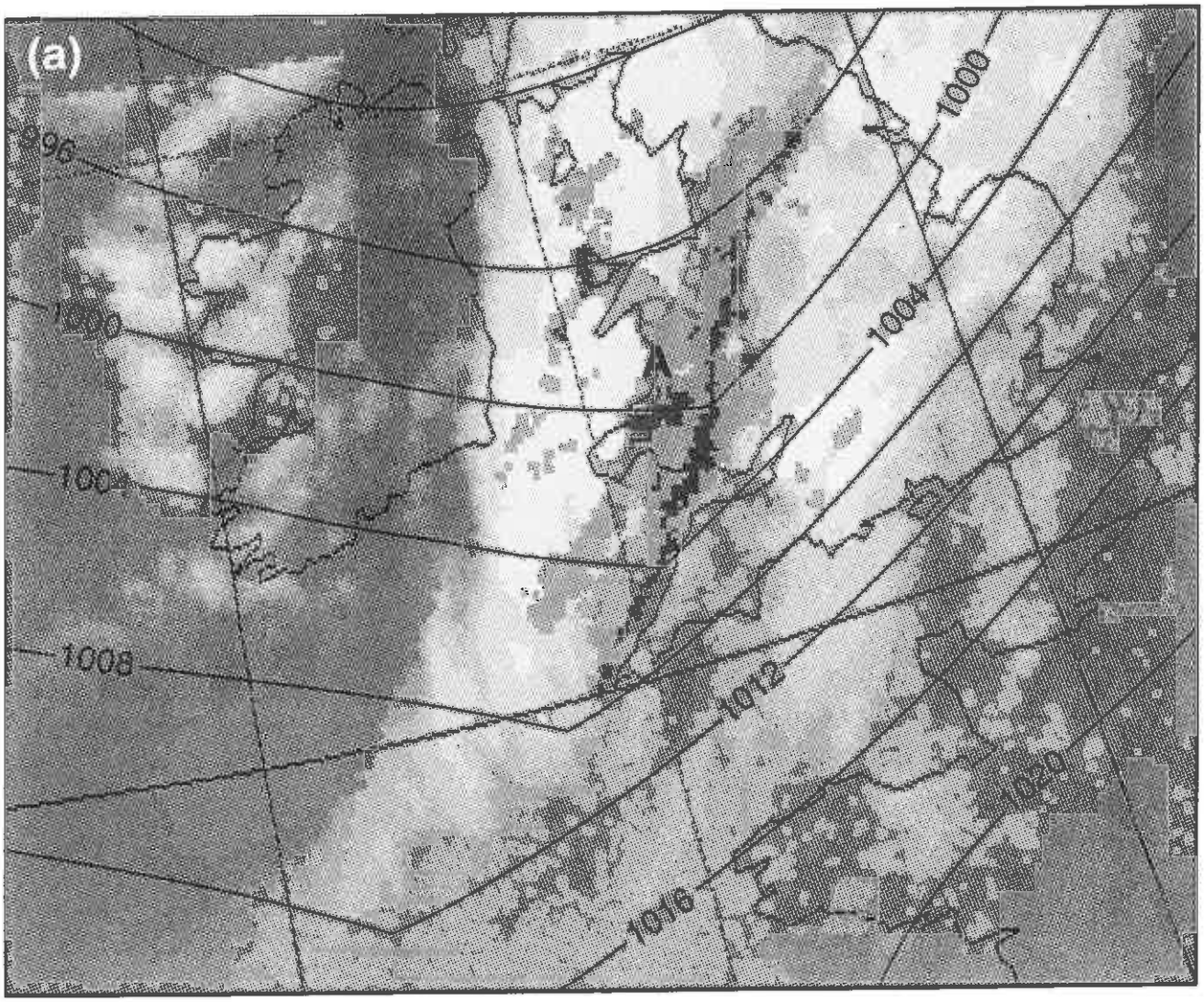

Fig 2(a)

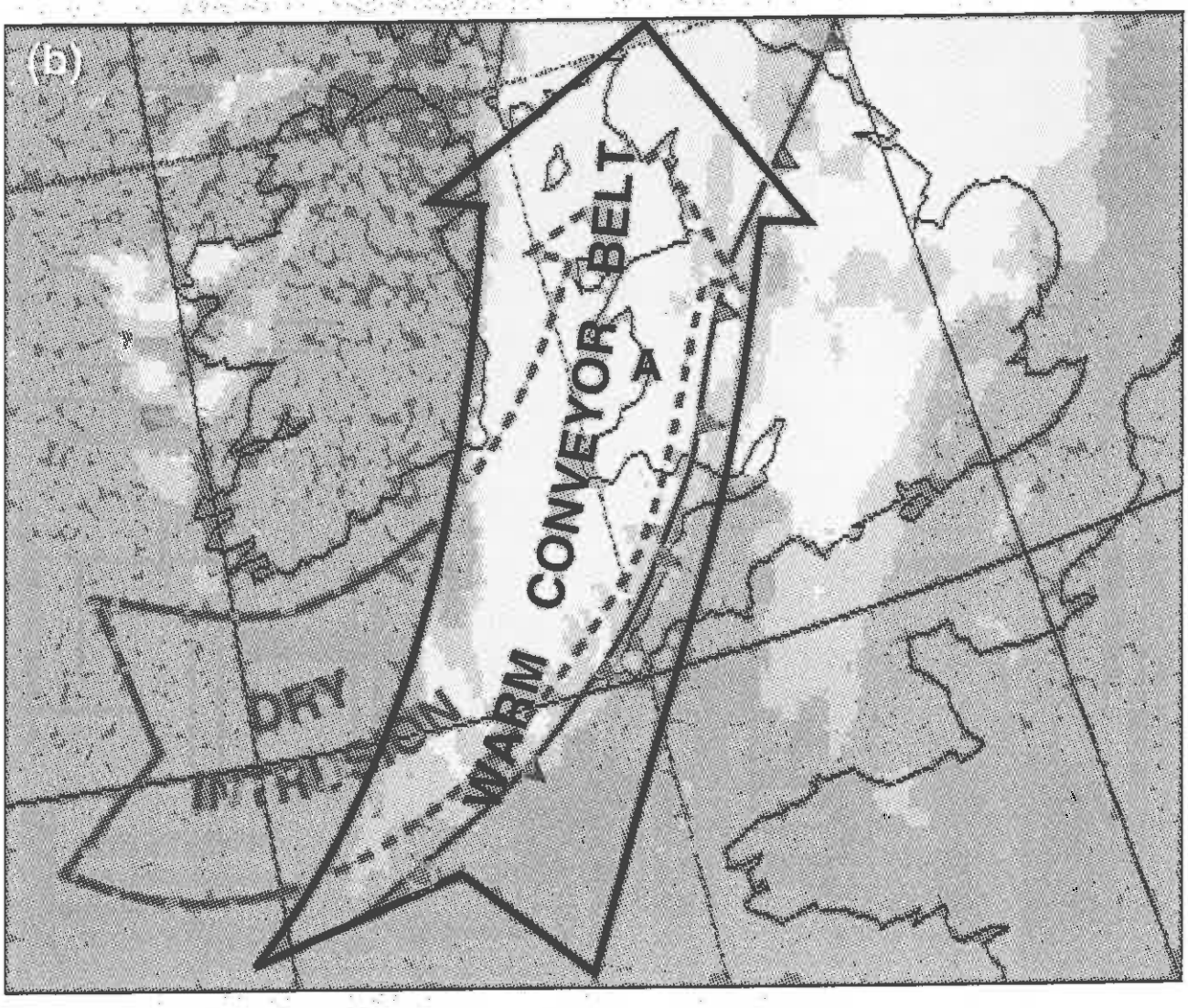

Fig 2(b)

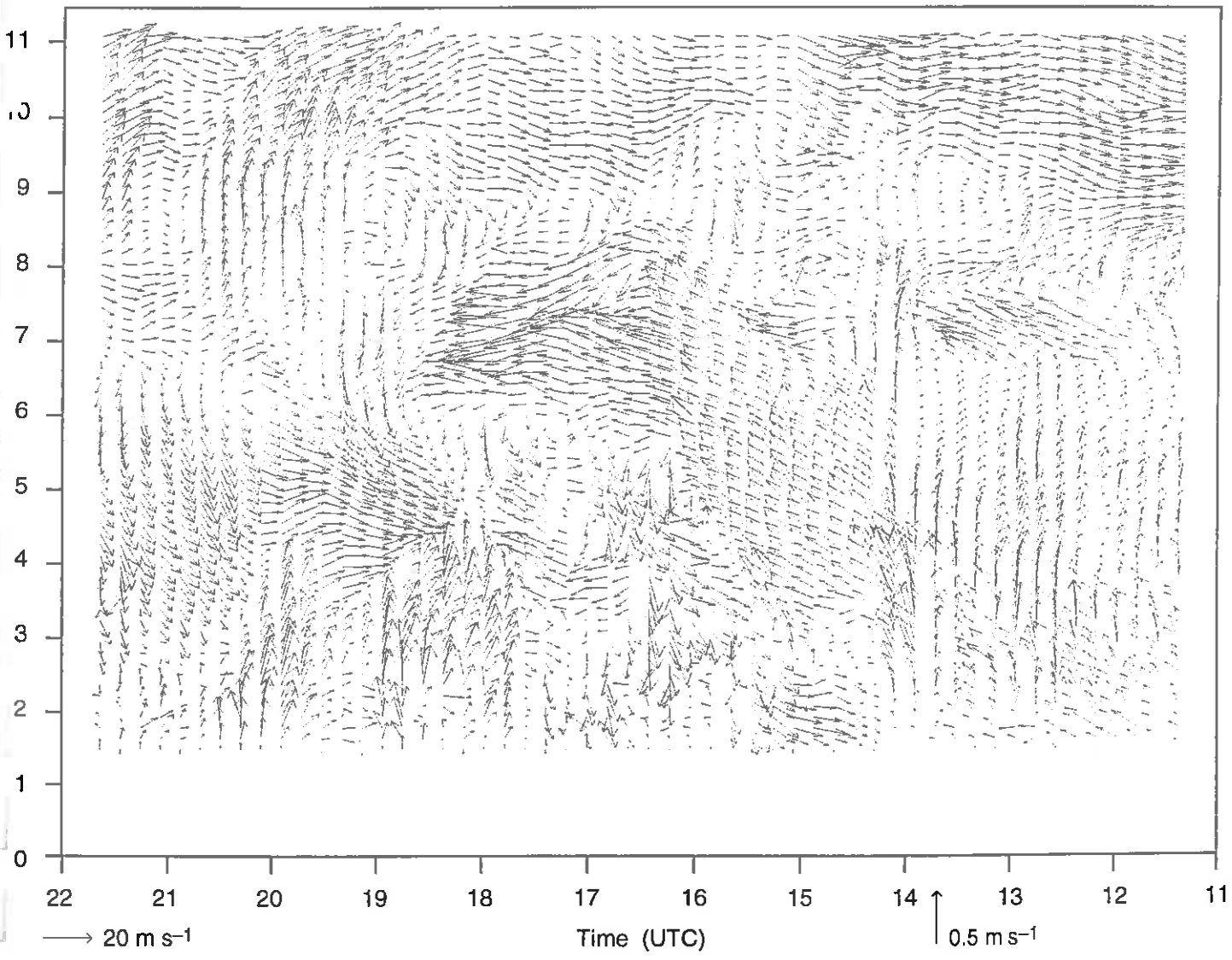
11
10
9
8
7
6
5
4
3
2
1
0
22
21
20
19
18
17
16
15
14
13
12
11
20 m s⁻¹
Time (UTC)
0.5 m s⁻¹

Figure 6.

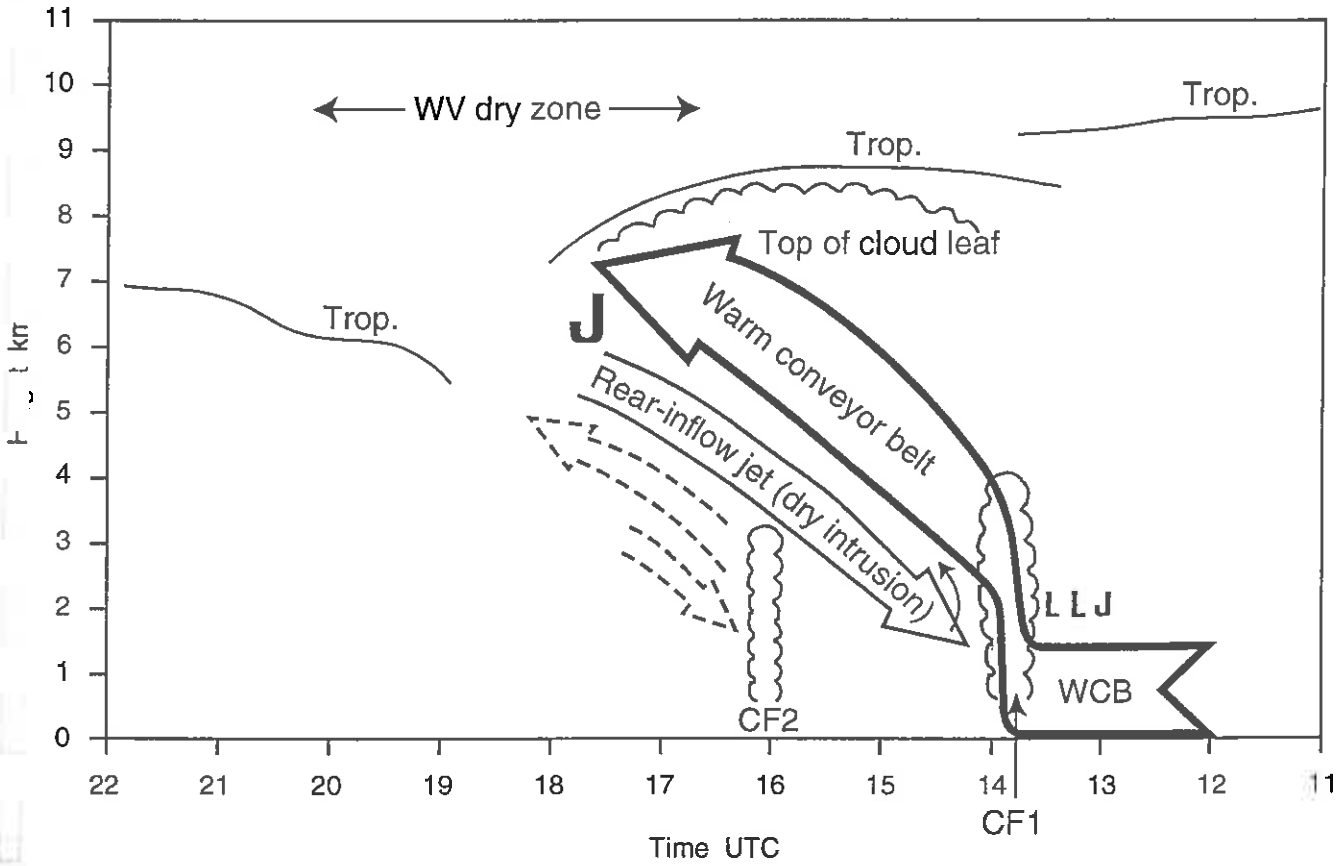

Figure 7. Synthesis of features identified in all previous figures.

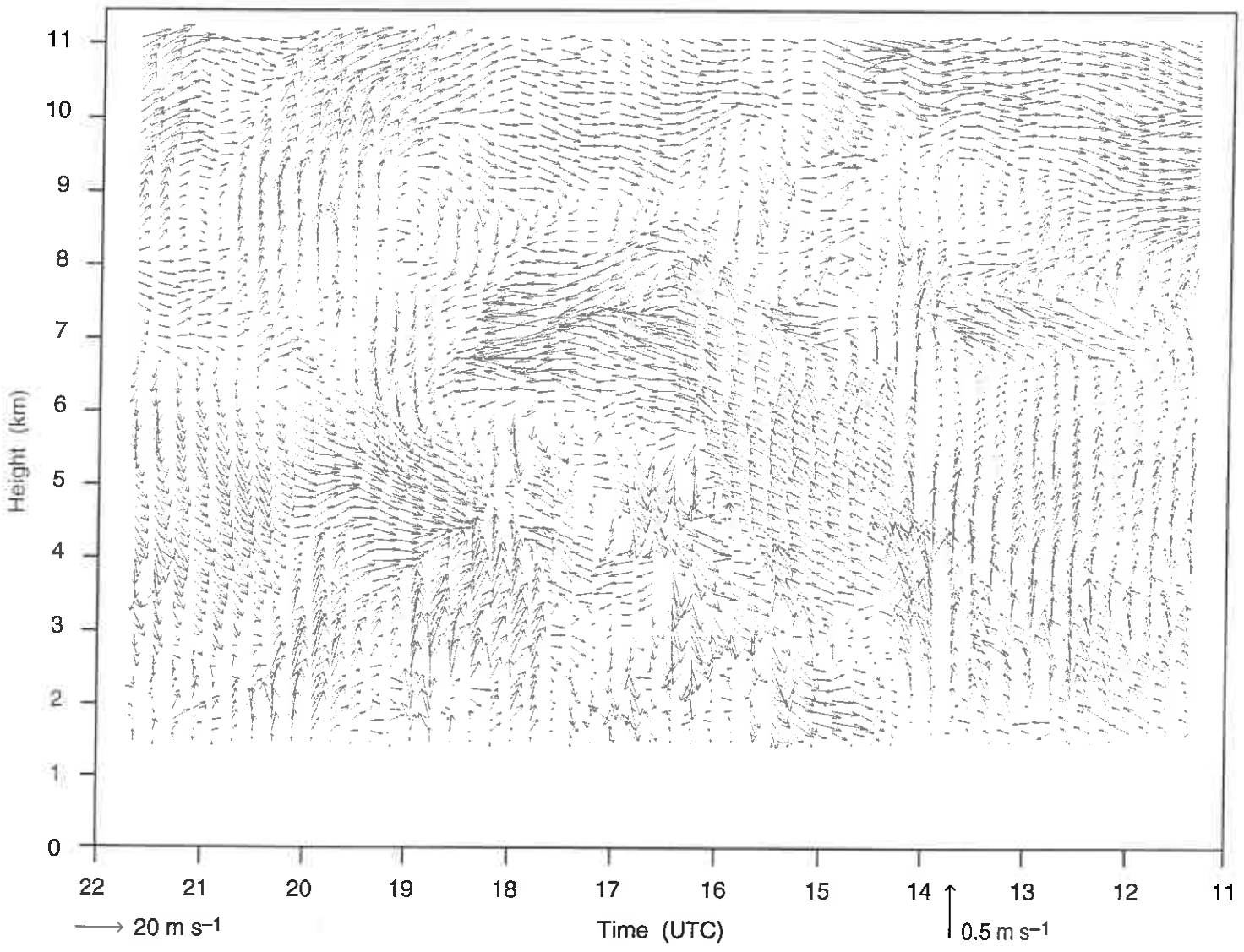
Height (km)
11
10
9
8
7
6
5
4
3
2
1
0
22
21
20
19
18
17
16
15
14
13
12
11
Time (UTC)
20 m s−1
0.5 m s−1

Figure 6.

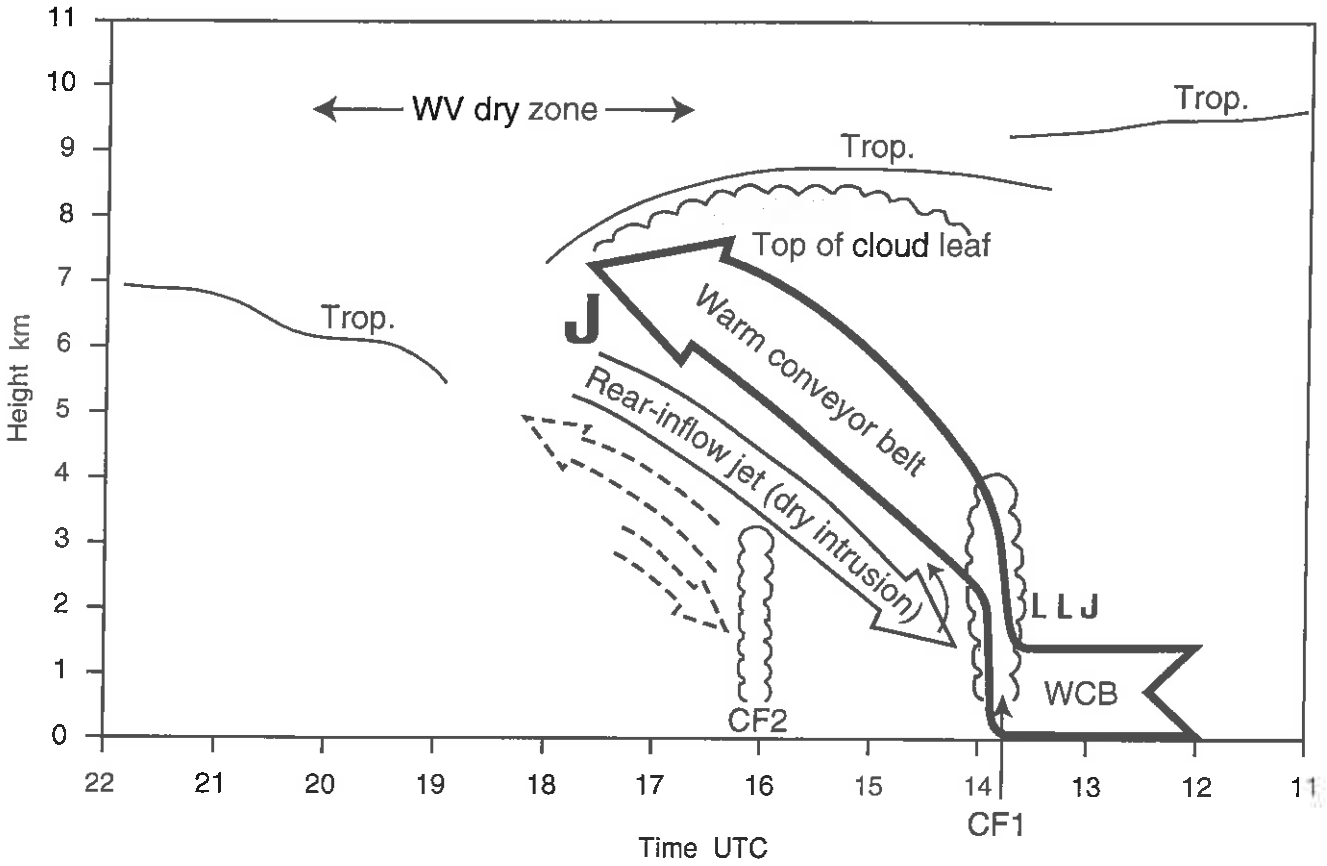

Figure 7. Synthesis of features identified in all previous figures.

CURRENT JCMM INTERNAL REPORTS

This series of JCMM Internal Reports, initiated in 1993, contains unpublished reports and also versions of articles submitted for publication. The complete set of Internal Reports is available from the National Meteorlogical Library on loan, if required.

1. **Research Strategy and Programme.**
   K A Browning et al
   January 1993

2. **The GEWEX Cloud System Study (GCSS).**
   GEWEX Cloud System Science Team
   January 1993

3. **Evolution of a mesoscale upper troposheric voriticity maximum and comma cloud from a cloud-free two dimensional potential vorticity anomaly.**
   K A Browning
   January 1993

4. **The Global Energy and Water Cycle**
   K A Browing
   July 1993

5. **Structure of a midlatitude cyclone before occlusion.**
   K A Browning and N Roberts
   July 1993

6. **Development in Systems and Tools for Weather Forecasting**
   K A Browning and G Szejwach
   July 1993

7. **Diagnostic study of a narrow cold frontal rainband and severe winds associated with a stratospheric intrusion.**
   K A Browning and R Reynolds
   August 1993

8. **Survey of perceived priority issues in the parametrizations of cloud-related processes GCMs**
   K A Browning
   September 1993

9. **The Effect of Rain on Longwave Radiation**
   I Dharssi
   September 1993

10. **Physical Cloud Microphyrocesses - A Description of the Parametrization used in the Large Eddy Model.**
H Swann
July 1994

11. **An Appreciation of the Meteorlogical Research of Ernst Kleinschmidt.**
A J Thorpe
May 1992

12. **Potential Vorticity of Flow Along the Alps**
A J Thorpe, H Volkert and Dietrich Heimann
August 1992

13. **The Representation of Fronts.**
A J Thorpe
January 1993

14. **A Parametrization Scheme for Symmetric Instability: Test for an Idealised Flow.**
C S Chan and A J Thorpe
February 1993

15. **The Fronts 92 Experiment: a Quicklook Atlas**
Edited by T K Hewson
November 1993

16. **Frontal wave satability during moist deformation frontogenesis. Part 1. Linear wave dynamics**
C H Bishop and A J Thorpe
May 1993

18. **Gravity waves in sheared ducts**
C Bishop and A J Thorpe
November 1993

19. **Potential Vorticity and Electroastatics Analogy: Quasi - Geostrophic Theory.**
C Bishop and A J Thorpe
November 1993

20. **Recent Advances in the Measurement of Precipitation by Radar.**
A J Illingworth - April 1993

21. **Micro-Physique et Givrage. Cloud Microphysics and Aircraft Icing.**
A J Illingworth May 1993

22. **Differential Phase Measurements of Precipitation.**
M Blackman and A J Illingworth
May 1993

23. **Estimation of Effective Radius of Cloud Particles from the Radar Reflectivity.**
N I Fox and A J Illingworth
May 1993.

24. **A Simple Method of Dopplerising a Pulsed Magnetron Radar.**
A Hau, A J Illingworth and J Eastment
November 1993.

25. **Radiation and Polar Lows.**
George C Craid
February 1994

26. **Collected preprints submitted International Symposium on the life Cycles of Ectratropical Cyclones; Bergen, Norway, 27 June - 1 July 1994**
April 1994.

27. **Convective Frontogenesis**
Douglas J Parker and Alan J Thorpe
April 1994

28. **Improved Measurement of the Ice Water Content in Cirrus Using a Total Water Evaporator.**
Philip R A Brown and Peter N Francis
April 1994

29. **Mesoscale Effects of Dry Intrusion within a vigorous Cyclone**
K A Browning and B W Golding
April 1994

30. **GEWEX Cloud System Study, Science Plan**
May 1994

31. **Parametrization of Mometum Transport by Convectively Generated Gravity Waves.**
R Kershaw
February 1995

32. **Mesoscale Modelling Newsletter, No5.**
May 1994

33. **Observations of the mesoscale sub-structure in the cold air of a developing frontal cyclone.**
K A Browning, S A Clough, C S A Davitt, N M Robertsf and T D Hewson
May 1994

34. **Longwave Radiative Forcing of a Simulated Tropical Squall Line**
Imtiaz Dharssi
July 1994

35. **On the nature of the convective circulation at a Kata-cold front**
K A Browning
September 1994

36. **Collective preprints of papers submitted to the COST-75 International Seminar on Advanced Weather Radar Systems, Brussels, 20-23 September 1994.**
November 1994

37. **Use of satellite imagery to diagnose events leading to frontal thunderstorms: Parts 1 and 11 of a case study.**
K A Browning and N M Roberts
November 1994

38. **The role of spaceborne millimeter-wave radar in the global monitoring of ice cloud.**
P R A Brown, A J Illingworth, A J Heymsfield, G M McFarquahar, K A Browning and M Gosset.
December 1994

39. **Potential Vorticity Inversion**
Michael Ziemianski
October 1994

40. **Theory of mature tropical cyclones; A comparison between Kleinschmidt (1951) and Emanual (1986)**
Suzanne L Gray
December 1994

41. **Dispersion and removal of pollutants during the passage of an atmospheric frontal System.**
N R Gimson
December 1994

54. **Parametrization of momentum transport by convection. I: Theory and cloud modelling results.**
P Kershaw and D Gregory
November 1995

55. **Variation of frontal structure along a cold front**
K A Browning and N M Roberts
November 1995

56. **Secondary Frontal Waves**
Douglas Parker
December 1995

57. **Objective Fronts**
T D Hewson
March 1996

58. **Mesoscale analysis of the activation of a cold front during cyclogenesis**
K A Browning, N M Roberts and A J Illingworth
June 1996

59. **Investigation of different representations of rain in a 1-d evaporation model**
H Swann
May 1996

60. **Parametrization of diabatic processes in the inversion of the omega-equation**
M Athanassiadou and A J Thorpe

61. **The role of the environmental flow in the development of secondary frontal cyclones.**
I A Renfrew, A J Thorpe and A Joly
June 1996

62. **Contributions to the AMS/RMS Conference on Mesoscale Processes Reading**
S Malardel, A J Thorpe and A Joly
June 1996

63. **Contributions to the AMS/RMS Conference on Mesoscale Processes Reading.**
9-13 September 1996
June 1996

64. **Vorticity and Potential Vorticity Stratified Flows Interacting with an Isolated Obstacle.**
Jorge A Gutierrez and A J Thorpe - September 1996

65. **Triple Point Development: Two Case Studies**
Douglas Parker
September 1996

66. **Radar observations of wind-shear splitting within evolving atmospheric Kelvin-Helmholtz billows**
D. Chapman and K.A.Browning
April 1997

67. **Cold Frontal Structure derived from radar wind profilers**
K.A.Browning, D. Jerrett, J.Nash, T.Oakley, N.M.Roberts
May 1997

Met Office Joint Centre for Mesoscale Meteorology Department of Meteorology
University of Reading PO Box 243 Reading RG6 6BB United Kingdom
Tel: +44 (0)118 931 8425 Fax: +44 (0)118 931 8791
www.metoffice.com